

## SYNTHESIS AND ELECTROCHEMICAL PROPERTIES OF ELECTROLYTES BASED ON PHOSPHONIUM, SULFONIUM AND IMIDAZOLIUM IONIC LIQUIDS FOR LI-ION BATTERIES

BARBORA GALAJDOVÁ, JAN ŽITKA, LUKÁŠ PAVLOVEC, OLGA TRHLÍKOVÁ,  
JANA KREDATUSOVÁ, and RAFAL KONEFAL

*Institute of Macromolecular Chemistry, Academy of Sciences of the Czech Republic, v.v.i, 162 00 Prague 6, Czech Republic  
gbarbora@seznam.cz*

This work describes synthesis and characterization of three ionic liquids (IL) with imidazolium, phosphonium or sulfonium cations. These ILs were used as precursors for the preparation of electrolytes by adding various types of lithium salts. Thermal and electrochemical properties of the electrolytes were studied to assess their feasibility for usage in lithium-ion batteries (LIB). Ethylmethylimidazolium phosphonic acid ethyl ester [EtMeIm]<sup>+</sup>[EtPITE]<sup>-</sup> with added Li salts showed very low conductivities of about 0.02 mS cm<sup>-1</sup> and a rather narrow electrochemical stability window of 4.3 V. Of all the ILs under study, this imidazolium-based IL exhibited the worst thermal properties both neat and with additional Li<sup>+</sup> salt. Therefore, using this IL as an electrolyte for LIB is unlikely. Methyltributylphosphonium bis(trifluoromethyl sulfonyl) imide [P<sub>1444</sub>]<sup>+</sup>[TFSI]<sup>-</sup> with Li salts had already significantly higher conductivities of 0.4–0.6 mS cm<sup>-1</sup> and showed a very wide electrochemical stability window of 7 V. TGA curves of [P<sub>1444</sub>]<sup>+</sup>[TFSI]<sup>-</sup> show excellent thermal stability up to 300 °C. DSC measurements showed semicrystalline behaviour of [P<sub>1444</sub>]<sup>+</sup>[TFSI]<sup>-</sup>; this unfavourable fact was overcome by the addition of Li<sup>+</sup> salts. Potential of this IL is very high for the use in LIB. At room temperature, trimethylsulfonium bis(trifluoromethyl sulfonyl) imide [S<sub>111</sub>]<sup>+</sup>[TFSI]<sup>-</sup> is a solid crystalline material, so it was mixed with [P<sub>1444</sub>]<sup>+</sup>[TFSI]<sup>-</sup>. The resulting mixture [P<sub>1444</sub>]<sup>+</sup>[S<sub>111</sub>]<sup>+</sup>[TFSI]<sup>-</sup> achieved the highest conductivities of 0.6–1.0 mS cm<sup>-1</sup> in comparison to other prepared ILs. The electrochemical stability is also interesting, its ESW value being 5.5 V. Thermal properties are comparable to those of [P<sub>1444</sub>]<sup>+</sup>[TFSI]<sup>-</sup>, but it does not show semicrystalline behaviour. This mixture is a promising electrolyte for LIB.

Keywords: ionic liquids, electrolyte, Li-ion battery, sulfonium, phosphonium

### Introduction

In recent years, lithium-ion batteries (LIBs) have been attracting attention as a storage system for “green” energy. Due to their wide range of applications, such as big electric vehicles (e.g., buses, electric cars), light electric vehicles (electric bikes, golf cart, small cars, forklifts), power tools (lawn mowers, electric saws, electric drills), remote control toys, wind energy storage and solar equipment, warning lights, UPS, small medical equipment, laptops, cell phones, etc., became one of the main areas of

interest in the scientific community. Like majority of batteries, also LIBs consist of four primary components: a cathode, an anode, an electrolyte, and a separator. In Table I, these essential components with their functions and general material are shown. Working principle of electrochemical reactions is described in Table II (ref.<sup>1</sup>).

During charging the battery, lithium based positive electrode releases some of its lithium ions, which move through the electrolyte to reach the negative electrode and remain there. At the same time, the electrons pass from the cathode to the anode through the external circuit to

Table I  
Essential component of Li-ion battery with their functions

Components	Operations	Materials
Cathode	Lithium ions enter the cathode when the battery discharges and leave when the battery charges	Lithium metal oxide powder
Anode	Lithium ions leave the anode when the battery discharges and enter the anode when the battery charges	Graphitic carbon powder
Electrolyte	The electrolyte allows the transport of lithium ions between the cathode and the anode but not electrons	Lithium salts and organic solvents
Separator	The separator prevents short circuit between the cathode and the anode and only lets lithium ions through pores	Microporous membranes

Table II  
Electrochemical reaction in Li-ion battery

Electrochemical reactions	
charge	
Cathode: $\text{LiMO}_2 \rightleftharpoons \text{Li}_{1-x}\text{MO}_2 + x\text{Li}^+ + x\text{e}^-$	
discharge	
charge	
Anode: $\text{C} + x\text{Li}^+ + x\text{e}^- \rightleftharpoons \text{Li}_x\text{C}$	
discharge	
charge	
Overall: $\text{LiMO}_2 + \text{C} \rightleftharpoons \text{Li}_x\text{C} + \text{Li}_{1-x}\text{MO}_2$	
discharge	

M = metal

maintain the overall neutrality. The battery stores energy during this process<sup>2</sup>.

Originally, the negative electrode material was lithium metal, but due to (i) creation of a dense surface film (which resulted in insufficient passivation), (ii) formation of lithium dendrites, (iii) safety issues, as well as (iv) a huge consumption of lithium, an investigation of novel materials is desirable<sup>3</sup>. Currently, as an anode material, graphite is mainly used, which has a low specific capacity and cannot meet the market demand for high-performance lithium batteries. Therefore, an extensive research aimed to optimize a negative electrode material was conducted. Comparative studies performed in order to find feasible anode material have been summarized and published, e.g.<sup>4,5</sup>. To provide a high energy capacity, the positive electrode must be capable to incorporate a large amount of lithium. Furthermore, the cathode materials must enable a reversible lithium-ion exchange with only small structural changes during the charge/discharge process to ensure a long cycle life. Other desirable properties are a high coulombic efficiency, insolubility in electrolyte, high lithium ions diffusivity and good electronic conductivity to exhibit high energy efficiency. They should also be prepared from inexpensive reagents applying low-cost syntheses. Commonly used cathode materials are Lithium Cobalt Oxide (LCO), Lithium Manganese Oxide (LMO), Lithium Iron Phosphate (LFP) and Lithium (Nickel-Manganese-Cobalt) Oxide (NMC)<sup>6</sup>.

Another fundamental component is the electrolyte, which allows the mobility of lithium ions. The choice of electrolyte has a significant impact on the safety and thermal stability of the battery. Commonly used organic electrolytes based on a combination of linear and cyclic alkyl carbonates are known and utilized due to their wide operating voltage. On the other hand, they pose a high volatility and flammability, which can result in serious safety risks. The main problem is their low flash and boiling point. Several studies were conducted on this topic<sup>7–10</sup>. Comparative summary of safety parameters of the most commonly used solvents and electrolytes are

shown in Table III. Measured components were dimethyl carbonate (DMC), ethylene carbonate (EC), diethyl carbonate (DEC), propylene carbonate (PC), 1-ethyl-3-methylimidazolium bis (trifluoromethanesulfonyl) imide (EMImNTf<sub>2</sub>), and 1-ethyl-3-methylimidazolium tetrafluoroborate (EMImBF<sub>4</sub>) together with lithium salts such as lithium tetrafluoroborate (LiBF<sub>4</sub>) and lithium hexafluorophosphate (LiPF<sub>6</sub>).

One of the main goals in the field of LIBs is therefore the development of new safer electrolytes<sup>11–13</sup>. Ionic liquids (ILs) are possible candidates for the substitution of commercial carbonate-based electrolytes<sup>14–17</sup>. ILs are salts which have a low melting point, below 100 °C (ref.<sup>18</sup>). They usually possess high chemical and thermal stabilities and extremely low or zero vapour pressure<sup>19</sup>. These qualities make room-temperature ionic liquids (RTILs) excellent candidates for use in a wide range of applications including electrochemical devices such as LIBs<sup>18</sup>. While ammonium-based ILs, such as imidazolium-, pyrrolidinium- and quaternary ammonium-based ILs, are the most widely studied ILs<sup>20</sup>, there is less interest in the phosphonium-based ILs. Some properties of both IL types are compared in several articles<sup>18,21,22</sup>. Even less attention has been paid to sulfonium-based ILs, mainly because of the lower stability of sulfonium salts in comparison to their imidazolium analogues<sup>23</sup>.

Therefore, based on limited knowledge of the behaviour and properties of sulfonium-based ILs, it was decided to synthesize three different types of cations [P<sub>1444</sub>]<sup>+</sup>, [EtMeIm]<sup>+</sup>, and [S<sub>1111</sub>]<sup>+</sup> and compare their thermal and electrochemical properties (Fig. 1). In addition, a necessary condition for conductivity of the IL-based electrolyte is a sufficient concentration of lithium ions. On the other hand, an added Li salt may increase the viscosity and thus decrease the electrolyte conductivity<sup>24</sup>. The influence of adding lithium salts, namely, lithium bis (trifluoromethyl sulfonyl) imide (LiTFSI), lithium bis (fluorosulfonyl) imide (LiFSI), lithium hexafluorophosphate (LiPF<sub>6</sub>) and lithium difluoro(oxalato)borate (LiDFOB) on the ionic conductivity and electrochemical

Table III

Safety parameters of solvents and electrolytes used in lithium-ion batteries: flash point  $F_p$ , self-extinguishing time SET, differential scanning calorimetry (DSC) peaks<sup>10</sup>

Solvent or electrolyte	$F_p$	SET	DSC peak [°C]		
	[°C]		1	2	3
DMC	23	*		160	160
1M LiPF <sub>6</sub> in DMC	23	*		97	97
1M LiBF <sub>4</sub> in DMC	23	17,7		100	
EC:DMC (50:50 wt.)	31	*	260	285	
1M LiPF <sub>6</sub> in EC:DMC (50:50 wt.)	23	51,5	80	190	268,5
DEC	28	*		202	
1M LiPF <sub>6</sub> in DEC	25	*		181	
1M LiBF <sub>4</sub> in DEC	29	*	150	185	
PC	58	*		290	
1M LiPF <sub>6</sub> in PC	65	55,7		219	235
1M LiBF <sub>4</sub> in PC	76	24,0		235	290
PC:EMImNTf <sub>2</sub> (60:40 wt.)	71	10,0		280	
1M LiPF <sub>6</sub> in PC:EMImNTf <sub>2</sub> (60:40 wt.)	78	8,0		235	270
1M LiBF <sub>4</sub> in PC:EMImNTf <sub>2</sub> (60:40 wt.)	91	4,0		280	
EC-PC (50:50 wt.)	72	*		270	
1M LiPF <sub>6</sub> in EC:PC (50:50 wt.)	69	10,0	230	260	280
1 M LiBF <sub>4</sub> in EC:PC (50:50 wt.)	91	66,0	85	245	290
EMImNTf <sub>2</sub>	215	0**		215	
EMImBF <sub>4</sub>	178	0**	140	185	
0.3 M LiPF <sub>6</sub> in EMImNTf <sub>2</sub>	121	0**		138	
0.3 M LiBF <sub>4</sub> in EMImNTf <sub>2</sub>	123	0**		255	
0.3 M LiPF <sub>6</sub> in EMImBF <sub>4</sub>	132	0**	130	210	262
0.3 M LiBF <sub>4</sub> in EMImBF <sub>4</sub>	118	0**	205	255	275

\* The system burnt off completely, \*\* non-flammable

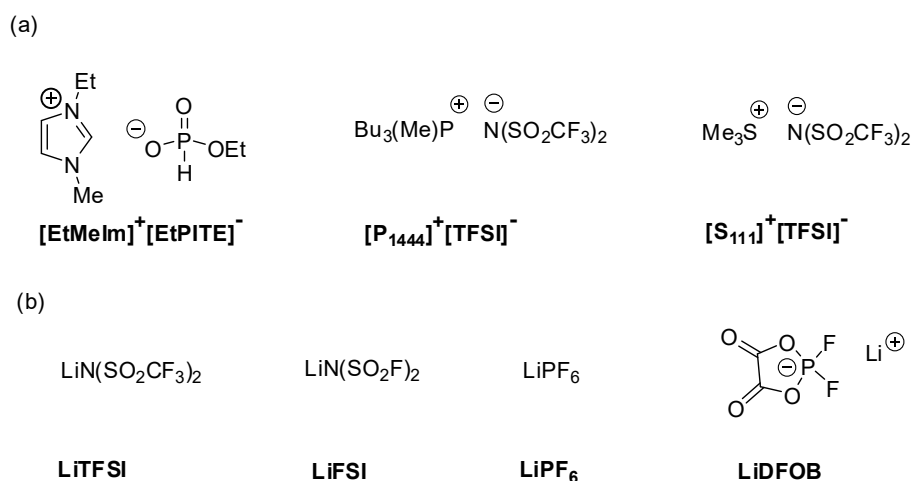


Fig. 1. Structures of synthesized ionic liquids (a) and lithium salts (b)

stability of the prepared IL was also determined. Those type of ILs were chosen for their unique composition.

## Experimental

### Chemicals

Tributylphosphine (97%, Sigma Aldrich), methyl iodide (99%, Acros), ethyl acetate (Lach Ner G.R.), *N*-methylimidazole (99%, Merck), diethyl phosphite (98%, Sigma Aldrich), triethyl phosphate (99.8% Sigma Aldrich), diethylether (Lach Ner G.R.) and methanol (Lach Ner G.R.) were used as received. Lithium bis(trifluoromethyl sulfonyl) imide (99%, abcr GmbH), lithium bis(fluorosulfonyl) imide (99%, Provisco), lithium hexafluorophosphate (99.9%, ABCR GmbH) and lithium difluoro(oxalato)borate (battery grade, Sigma Aldrich) were dried at 110 °C in vacuum for 48 h. Demineralized water was prepared by Millipore Elix 10 unit with resistivity 15 MΩ cm.

### Synthesis of methyltributylphosphonium bis(trifluoromethyl sulfonyl)imide $[P_{1444}]^+[TFSI]^-$

Methyl iodide (43 g, 0.3 mol) was added under stirring at room temperature (over a period of 1 h) to a solution of tributylphosphine (61 g, 0.3 mol) in methanol (150 mL) in a 250 mL three neck flask equipped with a thermometer and a reflux condenser. Then the mixture was refluxed for 3 hours. Methanol was distilled off in a rotary vacuum evaporator and a white solid methyltributylphosphonium iodide  $[P_{1444}]^+[I]^-$  was obtained. In the next step, a 5% solution of  $[P_{1444}]^+[I]^-$  in water (limited solubility in water) was mixed with a 10% aqueous solution of LiTFSI (a 5% excess in relation to  $[P_{1444}]^+[I]^-$ ). The obtained milky mixture was heated to approx. 80–90 °C for one hour which resulted in its separation into two phases. After cooling down, an oily bottom layer containing an ionic liquid with a bis(trifluoromethyl sulfonyl) imide anion  $[P_{1444}]^+[TFSI]^-$  was gathered, dissolved in ethyl acetate and washed 3 times with distilled water to remove traces of iodide.  $[P_{1444}]^+[TFSI]^-$  was then dried overnight under reduced pressure at 80 °C to remove residual water and ethyl acetate. Yield 84%.

### Synthesis of ethyl methylimidazolium phosphonic acid ethyl ester $[EtMeIm]^+[EtPITE]^-$

To a 500 mL 3-neck round bottom flask equipped with magnetic stirrer and reflux condenser, 0.5 mol (41.05 g) of *N*-methylimidazole and 0.5 mol (69.05 g) diethyl phosphite were added. The reaction was sealed under nitrogen and heated at reflux (190 °C) for 2 hours. The reaction mixture was then cooled down to RT and a viscous yellowish product was obtained. The product was washed three times with 250 mL of diethyl ether and

left for 24 hours in air. Afterwards the product was dried in a vacuum oven at 80 °C for 14 hours. Yield 87%.

### Synthesis of trimethylsulfonium bis(trifluoromethyl sulfonyl) imide $[S_{111}]^+[TFSI]^-$

Trimethylsulfonium iodide (100 g, 0.5 mol) was dissolved in 500 mL distilled water in a 1000 mL reagent bottle equipped with a magnetic stirrer. When the dissolution was completed, LiTFSI (172.25 g, 0.6 mol) dissolved in 500 mL of distilled water was added. The reaction mixture was stirred for 1 hour at 40 °C and then cooled down to RT. After that, two phases were obtained. An oily bottom layer containing an ionic liquid with a bis(trifluoromethyl sulfonyl) imide anion  $[S_{111}]^+[TFSI]^-$  was gathered and washed 3 times with distilled water to remove traces of iodide.  $[S_{111}]^+[TFSI]^-$  was dried overnight under vacuum at 80 °C to remove residual water. Yield 85%. After the drying procedure, the prepared ionic liquid became solid – white crystals were obtained. Physicochemical properties of the obtained plastic crystal are reported<sup>25</sup>. Due to its solid character,  $[S_{111}]^+[TFSI]^-$  was dissolved in  $[P_{1444}]^+[TFSI]^-$  at a 1:1 weight ratio to yield  $([P_{1444}]^+[S_{111}]^+[TFSI]^-)$ , i.e., 10 g of  $[S_{111}]^+[TFSI]^-$  and 10 g of  $[P_{1444}]^+[TFSI]^-$  were added to a 50 mL beaker with magnetic stirrer. After 48 hours a transparent liquid was observed. Mixing was done in a glovebox under argon atmosphere.

### Preparation of electrolyte

All electrolytes were prepared by the same procedure. To 15 mL vials equipped with a magnetic stirrer, 10 mL of ionic liquid and equivalent amount of dried lithium salts were added, which corresponded to 0.3 M concentration (Tab. IV). Electrolytes were prepared in a glovebox under argon atmosphere.

### NMR spectroscopy

<sup>1</sup>H NMR and <sup>31</sup>P NMR spectra were recorded with a Bruker Avance DPX 300 spectrometer operating at 300.1 and 121.5 MHz, respectively. NMR spectra were measured on the samples in 5 mm NMR tubes using

Table IV  
Electrolyte composition. The volume of the prepared electrolyte is 0.01 L and the molar concentration of Li<sup>+</sup> salt in electrolyte is 0.3 mol L<sup>-1</sup>

Li <sup>+</sup> salt	<i>M</i> [g mol <sup>-1</sup> ]
LiTFSI	287.09
LiFSI	187.07
LiDFOB	143.77
LiPF <sub>6</sub>	151.91

*M* = molecular weight of Li<sup>+</sup> salt used

methanol- $d_4$  as the solvent at 25 °C. Conditions for the  $^1\text{H}$  NMR measurements of the spectra were as follows:  $\pi/2$  pulse width 15.6  $\mu\text{s}$ , relaxation delay 10 s, acquisition time 4.95 s, 32 scans.  $^{31}\text{P}$  NMR was measured with pulse width 10.3  $\mu\text{s}$ , relaxation delay 10 s, acquisition time 0.67 s, 472 scans.

#### X-ray fluorescence

The samples were analysed with energy-dispersive X-ray fluorescence spectrometer SPECTRO XEPOS (SPECTRO Analytical Instruments, Germany), equipped with a silicon drift detector and excitation system with a 50 W Pd anode X-ray tube. The chamber was flushed with helium during the sample analyses. The Spectro Xepos software (TurboQuant method) was used for data analysis. Energy-dispersive X-ray fluorescence spectroscopy (XRF) was used to detect the presence or confirm the absence of iodine in the newly prepared ionic liquid.

#### Differential scanning calorimetry

Differential scanning calorimetry measurements were carried out on a DSC 8500 (Perkin Elmer) with nitrogen as a purge gas (20 mL  $\text{min}^{-1}$ ). The instrument was calibrated using indium as a standard. Samples of approximately 10 mg were encapsulated in aluminium pans. The DSC runs were performed in a cycle of heating-cooling-heating from  $-90$  °C to 100 °C at 10 °C  $\text{min}^{-1}$ . Glass transition temperature ( $T_g$ ) was determined from the heating run as the midpoint between the glassy and rubbery branches of the DSC trace.

#### Thermogravimetric analysis

Thermogravimetric analysis was recorded with Pyris 1 (Perkin Elmer), using the following TGA procedure: 5–10 mg of sample was heated at a constant heating rate of 10 °C  $\text{min}^{-1}$  under nitrogen flow of 30 mL  $\text{min}^{-1}$  from 30 °C to 650 °C.

#### Ionic conductivity

Ionic conductivity was measured by AC impedance spectroscopy using an Autolab 302N (Metrohm). Measurements were conducted in a PFA Swagelok cell containing 2 platinum and 2 glassy carbon electrodes at room temperature. The volume of the cell was approx. 4  $\text{cm}^3$ . Intervals for the frequency ranged between 1 Hz and 1 MHz applying a voltage amplitude of 0.1 V. The cell constant was determined using a standard solution of KCl, with a concentration range between  $5 \cdot 10^{-4}$  and  $1 \cdot 10^{-1}$  mol  $\text{L}^{-1}$  at 25 °C. The resistance (in  $\Omega$ ) was determined from the value of the real axis touchdown of the Nyquist plot, from which the conductivity (in  $\text{mS cm}^{-1}$ ) was calculated.

#### Cycling voltammetry

Cycling voltammetry (CV) was used to determine the electrochemical stability window (ESW). Cycling voltammetry (CV) measurements were performed using an Autolab 302N (Metrohm). Measurements were conducted in three electrodes system PFA Swagelok cells. Glassy carbon (Sigradur K, HTW,  $A = 0.189 \text{ cm}^2$ ) was used as a working and counter electrode. Silver wire was used as a quasi-reference electrode. The volume of the cell was approx. 1  $\text{cm}^3$ . ESW was determined as a potential of working electrode, applied current density was  $+200 \mu\text{A cm}^{-2}$ , resp.  $-200 \mu\text{A cm}^{-2}$ . Correction of the evaluated data was done by uncompensated resistance ( $R_u$ ) of electrolyte.  $R_u$  was measured in three electrode system using RLC bridge (Hameg Instruments).

## Results and discussion

#### NMR spectroscopy

Fig. 2 shows high-resolution  $^1\text{H}$  NMR (1a, 2a, 3a) and  $^{31}\text{P}$  NMR (1b, 2b, 3b) spectra of the ionic liquids prepared. The assignments of resonances to various proton types and the chemical structures are shown directly in each figure (1a, 2a, 3a). Part 1 describes the spectrum of a deuterated chloroform solution of  $[\text{EtMeIm}]^+[\text{EtPITE}]^-$ . The singlet at  $\delta = 10.7$  ppm was related to the methylene group among nitrogen atoms in the heterocycle (a). The multiplet signal of the other methylene groups from heterocycle (b, c) was observed at  $\delta = 7.4$  ppm. The strongest singlet signal at  $\delta = 4$  ppm belonged to methyl group bonded with nitrogen (d). Methylene group attached to nitrogen cation (e) was identified as a multiplet at  $\delta = 4.3$  ppm. A multiplet at  $\delta = 1.2$  ppm was assigned to methyl (f). Methylene attached to oxygen (g) had a similar multiplet signal as the methylene group attached to the nitrogen cation, but this signal was observed at  $\delta = 3.8$  ppm. A singlet signal at  $\delta = 1.5$  ppm was related to methyl group (h) bonded with methylene attached to oxygen. Hydrogen attached to phosphorus (i) exhibited two signals at  $\delta = 7.4$  and 6.4 ppm.

Part 2 shows the spectrum of deuterated methanol solution of  $[\text{P}_{1444}]^+[\text{TFSI}]^-$ . The multiplet signal of methylene groups attached to phosphorus (b) was observed at  $\delta = 2.12$  ppm, the characteristic doublet of methyl group bonded with phosphorus (a) was found at  $\delta = 1.73$  ppm. A multiplet at  $\delta = 1.49$  ppm was assigned to methylene protons (c, d) and a triplet at  $\delta = 0.96$  ppm was related to methyl group (e).

Part 3 describes the spectrum of a deuterated chloroform solution of  $[\text{S}_{111}]^+[\text{TFSI}]^-$  mixed with  $[\text{P}_{1444}]^+[\text{TFSI}]^-$  in a 1:1 wt. ratio. The primary difference between 2a and 3a is the strong singlet signal (f) at  $\delta = 2.9$  ppm, which was related to methyl groups attached to sulphur cation. This signal confirmed the presence of  $[\text{S}_{111}]^+[\text{TFSI}]^-$  in the prepared sample.

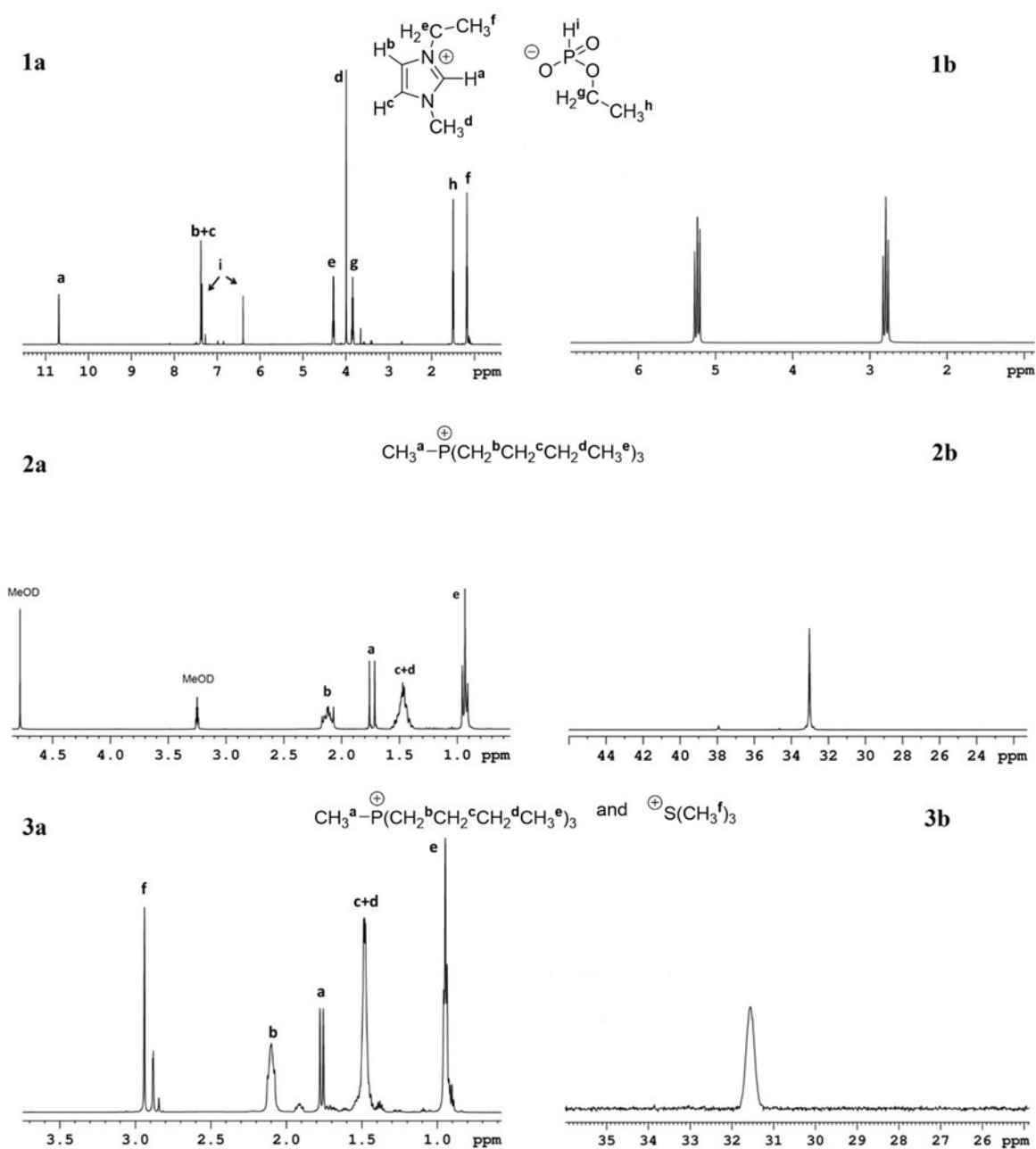


Fig. 2.  $^1\text{H}$  NMR spectra of cations  $[\text{EtMeIm}]^+$  (1a),  $[\text{P}_{1444}]^+$  (2a) and a mixture of  $[\text{P}_{1444}]^+$  with  $[\text{S}_{111}]^+$  (3a), and  $^{31}\text{P}$  NMR spectra of cations  $[\text{EtMeIm}]^+$  (1b),  $[\text{P}_{1444}]^+$  (2b) and a mixture of  $[\text{P}_{1444}]^+$  with  $[\text{S}_{111}]^+$  (3b)

$^{31}\text{P}$  NMR spectra of the prepared ionic liquids were shown in the second part (1b, 2b, 3b) of the figure. Strong signals at  $\delta = 33.0$  ppm and 31.5 ppm were assigned to phosphorus cation (1). The doublet of triplets observed at Part 1b appeared due to the pulse program of the experiment,  $^{31}\text{P}$  spectrum was measured without proton decoupling.

#### X-ray fluorescence

Iodine and other halogens can easily be oxidized in cells or batteries at high voltages<sup>26</sup> and therefore their presence in ionic liquids is undesirable. ED-XRF detected, of course, iodine in the initial compound  $[\text{P}_{1444}]^+[\text{I}]^-$  and it confirmed its absence in the newly prepared ionic liquid  $[\text{P}_{1444}]^+[\text{TFSI}]^-$  and  $[\text{S}_{111}]^+[\text{TFSI}]^-$  (Fig. 3).

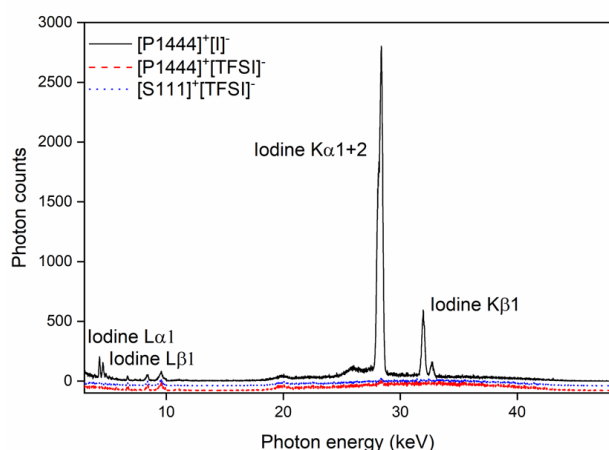


Fig. 3. Comparative XRF spectra of  $[P_{1444}]^+[TFSI]^-$ ,  $[S_{111}]^+[TFSI]^-$  and  $[P_{1444}]^+[I]^-$

### Thermal properties

The effects of adding  $Li^+$  salts into ILs on the thermal behaviour of the prepared mixtures were studied by differential scanning calorimetry. The first heatings are

depicted in Fig. 4. ILs  $[P_{1444}]^+[TFSI]^-$  and  $[P_{1444}]^+[S_{111}]^+[TFSI]^-$  showed semicrystalline behaviour with low melting temperatures, namely,  $16^\circ C$  and  $51^\circ C$ , respectively. Crystallization of ILs is undesirable for the usage in batteries. However, DSC measurements of their blends with  $Li^+$  salts revealed ionic interactions which caused amorphisation of the IL matrices. All of the used salts had a similar effect resulting in fully amorphous materials with  $T_g$  from  $-75^\circ C$  to  $-65^\circ C$  for  $[P_{1444}]^+[TFSI]^-$  and around  $-70^\circ C$  for  $[P_{1444}]^+[S_{111}]^+[TFSI]^-$  mixtures. Sample  $[EtMeIm]^+[EtPITE]^-$  was amorphous with  $T_g$  of  $-72^\circ C$  which was, by addition of  $Li^+$  salts, only slightly shifted to higher values (from  $-71^\circ C$  to  $-66^\circ C$ ). From this point of view all the prepared blends of ionic liquids with  $Li^+$  salts are suitable as electrolytes in batteries.

One of the mentioned advantages of ILs is their thermal stability. The thermal stability of pure IL and their blends with  $Li^+$  salts were verified by thermogravimetry (TGA), see Fig. 5. Both ILs with TFSI anion had a good thermal stability,  $[P_{1444}]^+[TFSI]^-$  is stable up to  $300^\circ C$ ,  $[P_{1444}]^+[S_{111}]^+[TFSI]^-$  up to  $250^\circ C$ . Ionic liquid  $[EtMeIm]^+[EtPITE]^-$  showed stability only to  $150^\circ C$  and the addition of  $Li^+$  salts did not improve it. The addition of  $Li^+$  salts had no influence on the thermal stability of  $[P_{1444}]^+[S_{111}]^+[TFSI]^-$  mixtures (stable up to  $250^\circ C$ ). However, ionic interactions of IL with  $Li^+$  salts had an impact on its

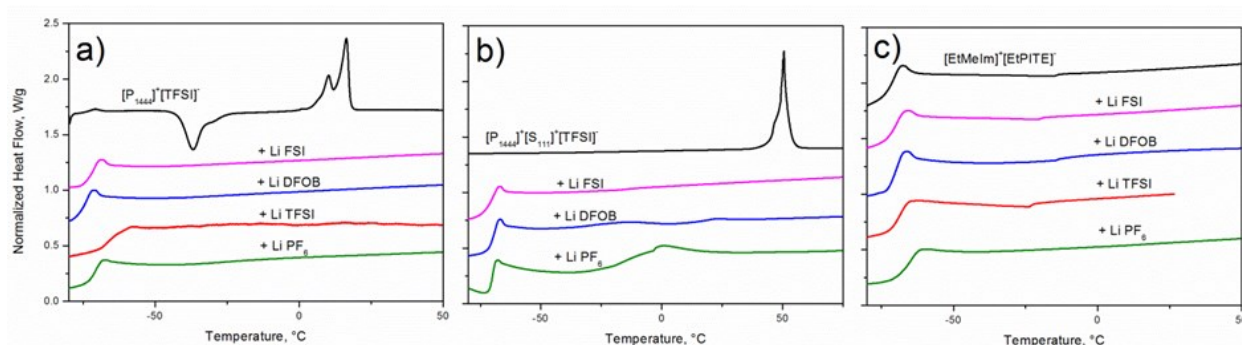


Fig. 4. DSC curves of ionic liquid matrixes (a)  $[P_{1444}]^+[TFSI]^-$ , (b)  $[P_{1444}]^+[S_{111}]^+[TFSI]^-$  (c)  $[EtMeIm]^+[EtPITE]^-$  and their mixtures with  $Li^+$  salts

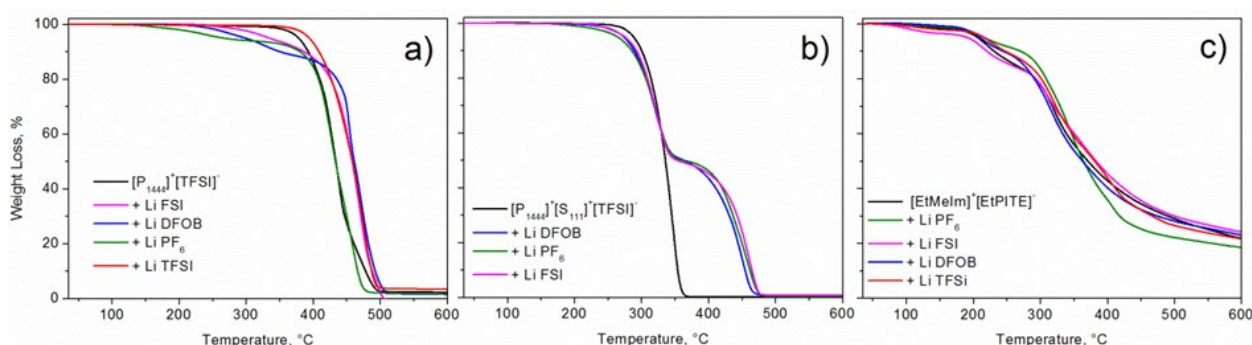


Fig. 5. TGA curves of ionic liquid matrixes (a)  $[P_{1444}]^+[TFSI]^-$ , (b)  $[P_{1444}]^+[S_{111}]^+[TFSI]^-$ , (c)  $[EtMeIm]^+[EtPITE]^-$  and their mixtures with  $Li^+$  salts

degradation at higher temperatures; it was shifted by about 120 °C to higher values. In the case of  $[P_{1444}]^+[TFSI]^- Li^+$ , salts slightly worsen thermal stability. But all mixtures except IL +  $LiPF_6$  were still stable up to 200 °C. The sample with  $LiPF_6$  showed no weight loss only up to 110 °C. This lower stability could be connected with high water content strongly bonded on  $LiPF_6$ . In conclusion, the ionic liquids prepared are thermally stable enough not to pose any danger of explosion in comparison to carbonate-based electrolytes, which were summarized in Table III.

### Ionic conductivity

In Table V ionic conductivities of the prepared ILs with different types of additional lithium salts in 0.3M concentration are shown. All of the samples were measured in the same cell and under the same conditions. Measurements were done at room temperature (25 °C); it is known that the performance of Li-ion batteries at elevated (>50 °C) and low (<-20 °C) temperatures is poor<sup>27</sup>.

$[EtMeIm]^+[EtPITE]^-$  exhibits poor conductivity properties with any of the Li salt used due to the high viscosity. Similar study with different imidazolium ionic liquids shows higher conductivity upon addition of lithium salts<sup>28</sup>, main difference being in the neat imidazolium ionic liquid used, which has a lower viscosity in comparison to our prepared  $[EtMeIm]^+[EtPITE]^-$ . On the other hand, our  $[P_{1444}]^+[TFSI]^-$  shows significantly higher conductivity contrary to similar phosphonium ionic liquid  $[P_{1444}]^+$  with different types of anion described in the literature<sup>29</sup>. ILs described in<sup>29</sup> possess ionic conductivity at 30 °C from  $7.8 \cdot 10^{-8}$  up to  $1.7 \cdot 10^{-4}$  S  $cm^{-1}$ , whereas our

Table V  
Ionic conductivities, highest achieved ionic conductivities are bolded in the table

Ionic liquid	Added salt <sup>a</sup>	Ionic conductivity <sup>b</sup> [mS $cm^{-1}$ ]
$[EtMeIm]^+[EtPITE]^-$	LiFSI	0.02
	LiDFOB	0.02
	LiTFSI	0.02
	<b>LiPF<sub>6</sub></b>	<b>0.03</b>
$[P_{1444}]^+[TFSI]^-$	LiFSI	0.50
	<b>LiDFOB</b>	<b>0.60</b>
	LiTFSI	0.45
	LiPF <sub>6</sub>	0.40
$[P_{1444}]^+[S_{111}]^+[TFSI]^-$	LiFSI	0.85
	<b>LiDFOB</b>	<b>1.00</b>
	LiTFSI	0.70
	LiPF <sub>6</sub>	0.65

<sup>a</sup> 0.3 M, <sup>b</sup> 25 °C

prepared  $[P_{1444}]^+[TFSI]^-$  exhibits at 25 °C ionic conductivity from  $0.3 \cdot 10^{-4}$  to  $6 \cdot 10^{-4}$  S  $cm^{-1}$ . A study done with phosphonium ionic liquids having a different alkyl chain length, as described in<sup>7</sup>, shows results comparable to those of ours. Electrochemical properties of various sulfonium ionic liquids were studied in<sup>30</sup>, yielding ionic conductivity results similar to those presented by us for sulfonium IL. In general, the highest ionic conductivity was observed in the mixture of  $[S_{111}]^+[TFSI]^-$  with  $[P_{1444}]^+[TFSI]^-$ , especially with LiDFOB; in this case the limit of 1 mS  $cm^{-1}$  was reached. LiDFOB in  $[P_{1444}]^+[TFSI]^-$  IL possesses higher ionic conductivity in comparison to other lithium salts used.

### Cycling voltammetry

Cyclic voltammetry is a method for evaluating the electrochemical behaviour of the system, where the current is recorded by sweeping the potential back and forth (from the positive to negative and *vice versa*)<sup>31</sup>. In this study we measured electrochemical window (ESW) for the chosen ILs, which exhibited the highest ionic conductivity. The narrowest ESW was observed at  $[EtMeIm]^+[EtPITE]^- + LiPF_6$  (Fig. 6 A); the value of ESW (4.3 V) lied at the lower limit of usage. It is suitable for the low voltage cathode, such as Lithium Iron Phosphate (LFP), Lithium Cobalt Oxide (LCO), or Lithium Manganese Oxide (LMO)<sup>1</sup>. Similar experiment with 1-alkyl-3-methylimidazolium ( $C_nMIM$ )<sup>+</sup> cations ( $n = 2$  to 6) with different anions [bis(trifluoromethylsulfonyl) imide (TFSI)<sup>-</sup>, hexafluorophosphate (PF<sub>6</sub>)<sup>-</sup>, tetrafluoroborate (BF<sub>4</sub>)<sup>-</sup>, and trifluoromethanesulfonate (TfO)<sup>-</sup>] shows wide range of ESW values. The widest ESW was observed for IL with PF<sub>6</sub> anion and the narrowest one for IL with TFSI anion; this means that the electrochemical stability is affected by the structure of the anion, highly fluorinated anions tending to be more stable against oxidation and reduction, see Table VI (cit.<sup>32</sup>).

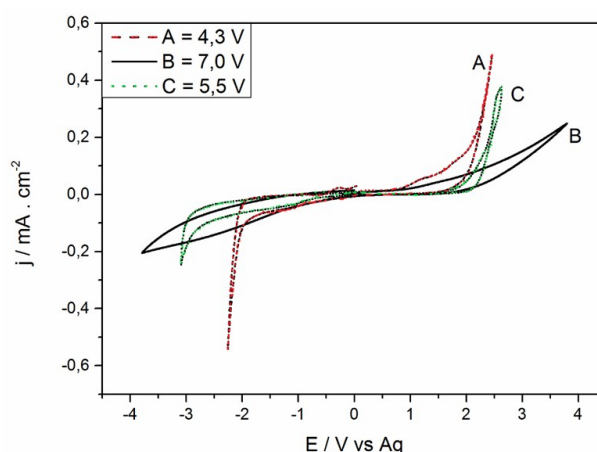


Fig. 6. Cycling voltammetry. A –  $[EtMeIm]^+[EtPITE]^- + LiPF_6$ , B –  $[P_{1444}]^+[TFSI]^- + LiDFOB$ , C –  $[P_{1444}]^+[S_{111}]^+[TFSI]^- + LiDFOB$

Table VI

Calculated values of the oxidation ( $E_{\text{ox}}^0$ ) and reduction ( $E_{\text{red}}^0$ ) potentials of the cations and anions of the ionic liquids vs. Li<sup>+</sup>/Li reference electrode, experimental electrode: GC – glassy carbon, Pt – platinum, W – wolfram

Ionic liquid	Cation		Anion		ESW (cycle method)	ESW experimental
	$E_{\text{ox}}^0$ [V]	$E_{\text{red}}^0$ [V]	$E_{\text{ox}}^0$ [V]	$E_{\text{red}}^0$ [V]		
[C <sub>2</sub> MIM] <sup>+</sup> [TFSI] <sup>-</sup>	6.072	-3.106	1.125	-7.523	4.232	4.5 (GC)
[C <sub>3</sub> MIM] <sup>+</sup> [TFSI] <sup>-</sup>	6.104	-3.317	1.087	-7.613	4.204	4.3 (GC)
[C <sub>4</sub> MIM] <sup>+</sup> [TFSI] <sup>-</sup>	6.131	-3.131	1.039	-7.723	4.169	4.6 (Pt)
[C <sub>2</sub> MIM] <sup>+</sup> [TfO] <sup>-</sup>	5.975	-3.033	1.685	-7.482	4.717	4.1 (Pt)
[C <sub>4</sub> MIM] <sup>+</sup> [BF <sub>4</sub> ] <sup>-</sup>	5.974	-2.973	3.851	-8.538	6.824	6.1 (W)
[C <sub>4</sub> MIM] <sup>+</sup> [PF <sub>6</sub> ] <sup>-</sup>	5.988	-3.005	4.987	-9.818	7.992	>7.1 (W)

Since [P<sub>1444</sub>]<sup>+</sup>[S<sub>111</sub>]<sup>+</sup>[TFSI]<sup>-</sup> + LiDFOB and [P<sub>1444</sub>]<sup>+</sup>[TFSI]<sup>-</sup> + LiDFOB show higher ESW, namely, 5.5 V and 7.0 V, respectively (Fig. 6 C, B), a novel high voltage cathode (e.g. LMNO) can be used. There is a potential for even higher ESW when more fluorinated anions are used; further experiments should be conducted.

## Conclusions

Syntheses of three ionic liquids (ILs) with imidazolium, phosphonium or sulfonium cations are described. Electrolytes were prepared by combining our synthesized ILs with the various types of Li salts. Electrochemical and thermal properties studied to assess the application of these IL as new types of electrolyte for lithium-ion batteries (LIB) were as follows.

- Ethylmethylimidazolium phosphonic acid ethyl ester [EtMeIm]<sup>+</sup>[EtPITE]<sup>-</sup> with added Li salts showed very low conductivities of about 0.02 mS cm<sup>-1</sup> and a rather narrow electrochemical stability window of 4.3 V. Imidazolium based IL with any of used Li salts exhibits poor thermal properties. Thus the use of this imidazolium IL as an electrolyte for LIBs seems to be unlikely.
- Methyltributylphosphonium bis(trifluoromethyl sulfonyl) imide [P<sub>1444</sub>]<sup>+</sup>[TFSI]<sup>-</sup> with Li salts had conductivities of 0.4–0.6 mS cm<sup>-1</sup> and a very wide electrochemical stability window of 7 V. TGA curves of [P<sub>1444</sub>]<sup>+</sup>[TFSI]<sup>-</sup> shows excellent thermal stability up to 300 °C. DSC measurements revealed semicrystalline behaviour of [P<sub>1444</sub>]<sup>+</sup>[TFSI]<sup>-</sup>; this unfavourable fact was overcome by the addition of Li salts. This IL has a high potential to be used in LIB.
- Trimethylsulfonium bis(trifluoromethyl sulfonyl) imide [S<sub>111</sub>]<sup>+</sup>[TFSI]<sup>-</sup> is a solid crystalline material, so that it was mixed with [P<sub>1444</sub>]<sup>+</sup>[TFSI]<sup>-</sup>. The resulting mixtures had very high conductivities of 0.6–1.0 mS cm<sup>-1</sup> in comparison to other prepared ILs and a rather wide electrochemical stability window of 5.5 V. Their thermal properties are comparable to those of [P<sub>1444</sub>]<sup>+</sup>[TFSI]<sup>-</sup> but do not exhibit the

semicrystalline behaviour. This mixture is therefore a promising electrolyte for Li-ion batteries.

*Special thanks go to the MEET Institute in Münster, FRG, for providing the equipment and sharing their knowledge.*

## Abbreviations

<i>c</i>	molar concentration (mol L <sup>-1</sup> )
CV	cyclic voltametry
[C <sub>n</sub> MIM] <sup>+</sup>	1-alkyl-3-methylimidazolium
DEC	diethyl carbonate
DMC	dimethyl carbonate
DSC	differential scanning calorimetry
$E_{\text{ox}}^0$	oxidation potential
$E_{\text{red}}^0$	reduction potential
EC	ethylene carbonate
EMImBF <sub>4</sub>	1-ethyl-3-methylimidazolium tetrafluoroborate
EMImNTf <sub>2</sub>	1-ethyl-3-methylimidazolium bis(trifluoromethanesulfonyl) imide
ESW	Electrochemical Stability Window
[EtMeIm] <sup>+</sup> [EtPITE] <sup>-</sup>	ethylmethylimidazolium diethylphosphite
$F_p$	Flash point
IL	ionic liquid
LCO	lithium-cobalt-oxide
LiDFOB	lithium difluoro(oxalato)borate
LFP	lithium iron-phosphate
LIB	lithium-ion battery
LiBF <sub>4</sub>	lithium tetrafluoroborate
LiFSI	lithium bis(fluorosulfonyl)imide
LiPF <sub>6</sub>	lithium hexafluorophosphate
LiTFSI	lithium bis(trifluoromethyl sulfonyl)imide
LMO	lithium-manganese-oxide
<i>M</i>	molar weight (g mol <sup>-1</sup> )
NMC	Nickel-Manganese-Cobalt Oxide
[P <sub>1444</sub> ] <sup>+</sup> [TFSI] <sup>-</sup>	methyltributylfosfonium bis(trifluoromethyl sulfonyl) imide
PC	propylene carbonate

[S <sub>111</sub> ] <sup>+</sup> [TFSI] <sup>-</sup>	trimethylsulfonium bis (trifluoromethyl sulfonyl)imide
SET	Self-Extinguishing Time
[TfO] <sup>-</sup>	trifluoromethanesulfonate
TGA	Termogravimetric analysis
T <sub>g</sub>	glass transition temperature (°C)
V	volume (L)
XRF	X-ray fluorescence

## REFERENCES

- Chen X., Shen W., Vo T. T., Cao Z., Kapoor A.: *10th International Power & Energy Conference (IPEC) 2012*, p. 230, Vietnam, Ho Chi Minh City. doi:10.1109/ASSCC.2012.6523269.
- Mathew M., Janhunen S., Rashid M., Long F., Fowler M.: *Energies* 11 (6), 1490 (2018). <https://doi.org/10.3390/en11061490>
- Nainville I., Lemarchand A., Badiali J. P.: *Electrochim. Acta* 41, 2855 (1996).
- Hui C., Shapter J. G., Yongying L., Gua G.: *J. Energy Chem.* 57, 451 (2021).
- Goriparti S., Miele E., De Angelis F., Di Fabrizio E., Zaccaria R. P., Capiglia C.: *J. Power Sources* 257, 421 (2014).
- Li W., Song B., Manthiram A.: *Chem. Soc. Rev.* 46, 3006 (2017).
- Lin X., Kaviani R., Lu Y., Hu Q., Shao-Horn Y., Grinstaff M. W.: *Chem. Sci.* 6, 6601 (2015).
- Roth E. P., Orendorff C. J.: *Electrochem. Soc. Interface* 21, 45 (2012).
- Hess S., Wohlfahrt-Mehrens M., Wachtler M.: *J. Electrochem. Soc.* 162 (2), A3084 (2015).
- Swiederska-Mocek A., Jakobczyk P., Rudnicka E., Lewandowski A.: *J. Mol. Liq.* 318, 113986 (2020).
- Blomgren G. E.: *J. Power Sources* 81-82, 112 (1999).
- Famprikis T., Canepa P., Dawson J. A., Islam M. S., Masquelier C.: *Nat. Mater.* 18, 1278 (2019).
- Wang J., Yamada Y., Sodeyama K., Watanabe E., Takada K., Tateyama Y., Yamada A.: *Nat. Energy* 3, 22 (2018).
- Galiński M., Lewandowski A., Stepniak I.: *Electrochim. Acta* 51, 5567 (2006).
- Francies C. F. J., Kyratzis I. L., Best A. S.: *Adv. Mater* 32, 1904205 (2020).
- Ye Y.-S., Rick J., Hwang B.-J.: *J. Mater. Chem. A* 1, 2719 (2013).
- Kar M., Simons T. J., Forsyth M., MacFarlane D. R.: *Phys. Chem. Chem. Phys.* 16, 18658 (2014).
- Girard G. M. A., Hilder M., Zhu H., Nucciarone D., Whitbread K., Zavorine S., Moser M., Forsyth M., MacFarlane D. R., Howlett P. C.: *Phys. Chem. Chem. Phys.* 17, 8706 (2015).
- Martins V. L., Sanchez-Ramirez N., Ribeiro M. C. C., Torresi R. M.: *Phys. Chem. Chem. Phys.* 17, 35 (2015).
- Pandian S., Raju S. G., Hariharan K. S., Kolake S. M., Park D. H., Lee M. J.: *J. Power Sources* 286 (2015).
- Tsunashima K., Sugiya M.: *Electrochem. Commun.* 9, 9 (2007).
- Seki S., Hayamizu K., Tsuzuki S., Fujii K., Umebayashi Y., Mitsugi T., Kobayashi T., Ohno Y., Kobayashi Y., Mita Y., Miyashiro H., Ishiguro S.-I.: *Phys. Chem. Chem. Phys.* 11, 3509 (2009).
- Zhao D., Fei Z., Ang W. H., Dyson P. J.: *Int. J. Mol. Sci.* 8, 4 (2007).
- Forsyth M., Girard G. M. A., Basile A., Hilder M., MacFarlane D. R., Chen F., Howlett P. C.: *Electrochim. Acta* 220 (2016).
- Anouti M., Caillon-Caravanier M., Dridi Y., Galiano H., Lemordant D.: *J. Phys. Chem. B* 112, 42 (2008).
- Woo J. J., Cha J. S., Hansung K., Jung H. Y.: *ACS Appl. Mater. Interfaces* 13, 6385 (2021).
- Kang X., Ding S. P., Jow T. R.: *J. Electrochem. Soc.* 149 (5), A586 (2002).
- McEwen A. B., Ngo H. L., LeCompte K., Goldman J. L.: *J. Electrochem. Soc.* 146 1687 (1999).
- Wu F., Schür A. R., Kim G.-T., Dong X., Kuenzel M., Diemant T., D'Orsi G., Simonetti E., De Francesco M., Bellusci M., Appetecchi G. B., Passerini S.: *Energy Storage Mater.* 42, 826 (2021).
- Yang L., Zhang Z.-X., Gao X.-H., Mashita K.: *J. Power Sources* 162, 614 (2006).
- Choudhary Y. S., Jothi L., Nageswaran G., in the book: *Spectroscopic Methods for Nanomaterials Characterizations* (Thomas S., Thomas R., Zachariah A. K., Mishra R. K., ed.), chapter 2, p. 19. Elsevier, Amsterdam 2017.
- Kazemiabnavi S., Zhang Z., Thorton K., Banerjee S.: *J. Phys. Chem. B* 120, 5691 (2016).